2012

Exergy Analysis of an Absorption Refrigeration System Using an Iconic Liquid as a Working Fluid in the Chemical Compressor

Yoon Jo Kim
yoonjo.kim@wsu.edu

Sarah Kim

Yogendra K. Joshi

Andrei G. Fedorov

Paul A. Kohl

Exergy Analysis of an Absorption Refrigeration System Using an Ionic Liquid as a Working Fluid in the Chemical Compressor

Yoon Jo KIM[1]*, Sarah KIM[2], Yogendra JOSHI[3], Andrei FEDOROV[3], and Paul KOHL[2]

[1]Washington State University, Department of Mechanical Engineering,
Vancouver, WA 98686, USA

[2]Georgia Institute of Technology, School of Chemical and Biomolecular Engineering,
Atlanta, GA 30332, USA

[3]Georgia Institute of Technology, G.W. Woodruff School of Mechanical Engineering,
Atlanta, GA 30332, USA

ABSTRACT

The first and second law of thermodynamics are applied to an ionic-liquid (IL) based absorption refrigeration system for high power electronics cooling. The IL is a salt in a liquid state usually with an organic cation and inorganic anion. It provides an alternative to the normally toxic working fluids used in the chemical compression loop, such as ammonia in conventional absorption systems. The use of ILs also eliminates crystallization and metal-compatibility problems of the water/LiBr system. In this study, mixtures of refrigerants and imidazolium-based ILs are theoretically explored as the working fluid pairs in a miniature absorption refrigeration system, so as to utilize waste-heat to power a refrigeration/heat pump system for electronics cooling. A mathematical model based on exergy analysis is employed to characterize the performance for specific refrigerant/IL pairs. Both the coefficient of performance (COP) and the exergetic coefficient of performance (ECOP) of the absorption system and components are evaluated. The thermodynamic properties of ILs are evaluated using the correlations based on group contribution methods. A non-random two-liquid (NRTL) model is built and used to predict the solubility of the mixtures. The properties of the refrigerants are determined using REFPROP 6.0 software. Saturation temperatures at the evaporator and condenser are set at 25^{o}C and 50^{o}C, respectively. The power dissipation at the evaporator is fixed at 100 W with the operating temperature set at 85^{o}C, which are the benchmark conditions for high performance microprocessor chip cooling. The desorber and absorber outlet temperatures are adjusted to evaluate the system performance variation with respect to the operating condition change. The effect of the refrigerant/IL compatibility, alkyl chain length of the IL cation, and thermodynamic properties of the refrigerants, such as latent heat of evaporation, on the ECOP is investigated. Also the exergy destruction of each component of the cycle is evaluated and discussed as a means to identify the critical component(s) of the system that would require optimization.

1. INTRODUCTION

Recent advances in semiconductor technologies have led to an increase in power density for high performance chips, such as microprocessors. According to the International Technology Roadmap for Semiconductors (ITRS), these chips are expected to dissipate an average heat flux as high as 75 W/cm^2, with the maximum junction temperature not exceeding 85^{o}C, in 2012, while in 2024 the numbers are more challenging, 120 W/cm^2 and 70^{o}C, respectively (ITRS 2005). Conventional chip packaging solutions, which use air-cooling, face difficulties in dissipating such high heat fluxes in the limited space allocated to thermal management.

A variety of novel alternative thermal solutions for electronics cooling have been reported, including thermosyphon (Pal et al., 2002), loop heat pipes (Maydanik et al., 2005), electroosmotic pumping (Jiang et al., 2002), stacked micro-channels (Wei and Joshi, 2004), impinging jets (Bintoro et al., 2005), thermoelectric micro-coolers (Fan et al., 2001), vapor compression refrigeration (Mongia et al., 2006) and absorption based refrigeration systems (Drost and Friedrich, 1997; Kim et al., 2008). These cooling systems can be categorized into passive system and active system. Passive cooling system utilizes capillary or gravitational buoyancy force to circulate working fluid, while active cooling system is driven by a pump or a compressor for augmented cooling capacity and improved performance.

Also, an active system driven by the compressor can be called refrigeration system which may offer further increase in power by insertion of a negative thermal resistance into heat flow path (Mongia et al., 2006).

Ionic liquids (ILs), which are salts in a liquid state usually with organic cations and inorganic anions, are used as an absorbent fluid in a miniature absorption refrigeration system designed for current electronic cooling requirements. ILs have the character of molten salts, which are moisture and air stable at room temperature. Most ILs are thermally stable to temperatures well above those in vapor compression refrigeration systems, > 400 K (Heintz et al., 2003; Scammells et al., 2004; Wilkes, 2004; Hagiwara and Ito, 2005). However, in the case of a prolonged exposure to elevated temperatures, the effective decomposition temperature could be lower. Blake et al. (2006) reported that the half-life of [bmim][PF_6] is only 138 days at 573K, while at 423 K (the highest operating temperature of an absorption system), it could be more than 10 years. Since the degradation products of ILs are often volatile compounds (Scammells et al., 2004), the operating temperature needs to be kept within acceptable limits. Due to the toxic and flammable nature of volatile organic compounds (VOCs) (Cull et al., 2000), ILs with the negligible vapor pressure have been considered as a possible replacements of solvents for organic synthesis (Wasserscheid and Keim, 2000), biphasic catalysis, separation and extraction processes (Huddleston et al., 1998), and dissolution of biomaterials (Swatloski et al., 2002). Thus, even though some ILs may not be intrinsically "green", they can be designed to be environmentally benign, with large potential benefits for sustainable chemistry (Rogers and Seddon, 2003).

With the above mentioned features of ILs such as tunable properties, zero vapor pressure, and high thermal stability, ILs are promising absorbents (Shiflett and Yokozeki, 2006b). In particular, the low volatility of the IL enables easy separation of the volatile working fluid from the IL by thermal stratification with the minimum harmful impacts on environment (Kim et al., 2011a). ILs can provide an alternative to the normally toxic working fluids used in some absorption systems, such as the ammonia/water system. Since many of the ILs have melting points below the lowest solution temperature in the absorption system (~300 K) (Dzyuba and Bartsch, 2002; Marsh et al., 2004; Troncoso et al., 2006; Valkenburg et al., 2005; Huddleston et al., 2001), they also eliminate the crystallization and metal-compatibility problems of the water/LiBr system. Several theoretical works on the absorption refrigeration system using ILs as absorbent have been reported (Shiflett and Yokozeki, 2006a; Shiflett and Yokozeki, 2006b; Kim et al., 2011; Yokozeki, 2005; Shiflett and Yokozeki, 2007; Kim et al., 2011b). Comprehensive thermodynamic analysis has been conducted to explore the feasibility and compatibility of IL/refrigerant mixtures as the working fluid of an absorption system (Kim et al., 2012) and Kim et al. (2011a) built and first IL absorption system prototype and experimentally demonstrated and measured the performance.

In this study, the first and second law of thermodynamics were applied to an ionic-liquid based absorption refrigeration system for high power electronics cooling to determine the coefficient of performance (COP) and the exergetic coefficient of performance (ECOP) of the system. The mixtures of imidazolium IL, [bmim][PF_6], and several HFC refrigerants, R125 (pentafluoroethane), R134a (1,1,1,2-tetrafluoroethane), R143a (1,1,1-trifluoroethane), R152a (1,1-difluoroethane), and R32 (difluoromethane) were considered as the working fluids of the system. Water, which is attractive due to its high thermal conductivity and latent heat of evaporation, was also explored as a refrigerant with the IL, [emim][BF_4]. The saturation temperatures at the evaporator and condenser were set at 25^{o}C and 50^{o}C, respectively, with the power dissipation of 100 W and 85^{o}C chip temperature.

2. SYSTEM ANALYSIS

2.1 IL Absorption System

Fig. 1 shows a schematic diagram of a thermally driven absorption refrigeration system using a refrigerant/IL mixture as a working fluid pair. The system consists of an evaporator, an absorber, a desorber, a condenser, a liquid pump, and an expansion device. One of the major advantages of the absorption refrigeration system is the utilization of waste heat, which can have temperature of 90^{o}C or lower. The use of waste heat results in a significant reduction in operating cost and justifies the added balance-of-plant for the absorption refrigeration system. Furthermore, the only component of this system with moving mechanical parts is the liquid pump, so that relatively quiet operation is possible with no lubrication needed. In general, the key system performance metric, coefficient of performance (COP), is defined as the heat removed at the evaporator per total power supplied to the system, Equation 1.

$$\mathrm{COP} = \frac{Q_e}{Q_d + W_p} \approx \frac{Q_e}{Q_d} \tag{1}$$

where W_p and Q are pumping work and the heat input/output, respectively. The subscripts "e" and "d" denote the evaporator and desorber, respectively. Since the heat supply at the desorber is from waste heat (i.e., it is essentially

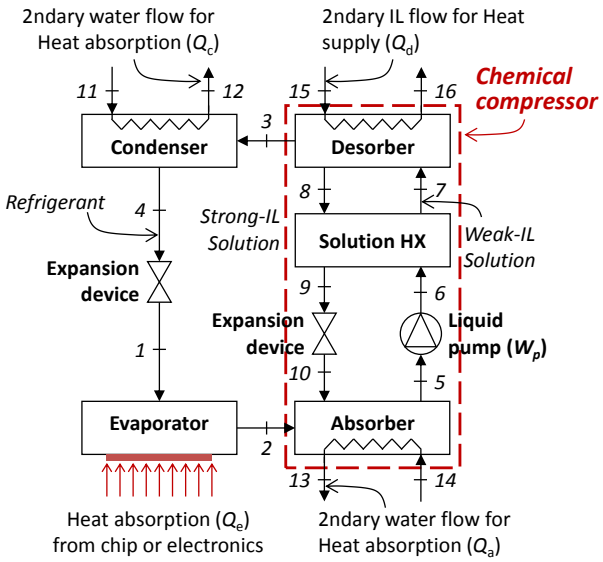

Figure 1: Schematic diagram of an absorption refrigeration system using IL/refrigerant mixture as a working fluid pair.

free), a more relevant coefficient of performance (COP_{waste}) can be defined by eliminating Q_d from Eq. 1, i.e., $COP_{waste} = Q_e / W_p$.

The cyclic process for the refrigerant loop is the same as that of a vapor compression system, except the mechanical compressor is replaced with a '*chemical compressor*' which consists of an absorber, liquid pump, solution heat exchanger, desorber and expansion device. The pressurization process in the chemical compressor starts in the absorber, where the refrigerant vapor from the evaporator (state point 2) is exothermically absorbed into the weak (refrigerant) solution (state point 10), resulting in strong (refrigerant) solution at state point 5. Once the refrigerant is absorbed, the solution is pressurized by the liquid pump. The solution heat exchanger preheats the strong solution of state point 6 to state point 7 using the high temperature weak solution flow from the desorber. A high pressure and high temperature superheated refrigerant vapor is generated in the desorber and the refrigerant is endothermically desorbed from the strong solution. The refrigerant vapor returns to the refrigerant loop. Meanwhile, the mixture solution becomes the weak solution and returns to the absorber through solution heat exchanger and expansion device in sequence, which completes the solution loop or chemical compression cycle. The condensation/absorption process at the absorber and vaporization/desorption process at the desorber make it possible to use a low-power-input liquid pump to increase the pressure between the condenser and the evaporator. Although the presence of the absorber and desorber increases the overall system volume, the displacement volume and power consumption for compression of the liquid are much smaller than those for vapor compression. Also, the slight modification of the absorption refrigeration system can be used for power cycles, e.g., the Kalina cycle (Ibrahim and Klein, 1996; Xu et al., 2000; Sun, 2000) and a heat transformer (Rivera et al., 2011).

2.2 IL Thermodynamic and Thermophysical Properties

The correlations of the refrigerant/IL mixture properties developed based on non-random two-liquid (NRTL) activity coefficient model by Shiflett and Yokozeki (2006b) are used in this study, Equations 2 and 3.

$$\ln \gamma_m = x_n^2 \left[\tau_{nm} \left(\frac{F_{nm}}{x_m + x_n F_{nm}} \right)^2 + \frac{\tau_{nm} F_{nm}}{\left(x_n + x_m F_{mn} \right)^2} \right] \tag{2}$$

$$\ln \gamma_n = x_m^2 \left[\tau_{mn} \left(\frac{F_{mn}}{x_n + x_m F_{mn}} \right)^2 + \frac{\tau_{mn} F_{mn}}{\left(x_m + x_n F_{nm} \right)^2} \right] \tag{3}$$

where x is the liquid-phase mole fraction and γ represents the activity coefficients. The subscripts "m" and "n" denote the refrigerant and the IL, respectively. F is an adjustable binary interaction parameter and τ are defined in Equations 4 and 5.

Table 1: Adjustable parameters in Eq. 5.

Working fluid pair (1)/(2)	τ_{mn}^{0} [-]	τ_{mn}^{1} [K]	τ_{nm}^{0} [-]	τ_{nm}^{1} [K]
R134a/[emim][Tf_2N][a]	6.6710	-716.04	-0.8502	-262.85
R134a/[bmim][PF_6][a]	1.2510	411.45	0.57596	-406.43
R134a/[hmim][Tf_2N][a]	13.186	-2904.5	-5.3330	1128.9
R134a/[hmim][BF_4][a]	7.5975	-1176.7	-0.26344	-275.97
R134a/[hmim][PF_6][a]	11.718	-2397.7	-3.5270	688.02
Water/[emim][BF_4][b]	17.253	-6445.4	-12.650	4426.8

[a] Ren and Scurto, 2006; [b] Seiler et al., 2004

$$F_{mn} \equiv \exp\left(-\omega\tau_{mn}\right) \quad \text{and} \quad F_{nm} \equiv \exp\left(-\omega\tau_{nm}\right) \tag{4}$$

$$\tau_{mn} \equiv \tau_{mn}^{0} + \frac{\tau_{mn}^{1}}{T} \quad \text{and} \quad \tau_{nm} \equiv \tau_{nm}^{0} + \frac{\tau_{nm}^{1}}{T} \tag{5}$$

Where T is absolute temperature, respectively, and ω = 0.2. The parameters, τ_{mn}^{0}, τ_{mn}^{1}, τ_{nm}^{0}, and τ_{nm}^{1}, have been determined based on literature vapor-liquid equilibrium (VLE) data, as shown in Table 1. It is assumed that upon mixing, the refrigerant/IL mixtures are only physically interacting. To the best knowledge of the authors, no chemical reactions between the substances have been reported. The predicted mole fractions using the NRTL model are compared with the measured mole fraction data in references (Ren and Scurto, 2006; Seiler et al., 2004) in Fig. 2, which shows good agreement between the measured and predicted data. The correlations based on group contribution methods were used to evaluate the viscosity (Gardas and Coutinho, 2009), specific heat (Gardas and Coutinho, 2008) and density (Jacquemin et al. 2007) of the ILs. The REFPROP 6.0 software (McLinden et al., 1998), developed by the National Institute of Standards and Technology, has been used to calculate the thermodynamic and transport properties of the refrigerants. It implements three models for the thermodynamic properties of pure fluids: (i) equations of state explicit in the Helmholtz energy, (ii) the modified Benedict-Webb-Rubin equation of state, and (iii) an extended corresponding states (ECS) model. (McLinden et al., 1998)
The specific enthalpy, h_{IL}, and specific entropy, s_{IL}, of ILs were calculated using Equations 6 and 7. (Smith et al. 2000)

$$h_{IL} = \int_{T_0}^{T} c_{p,IL}\, dT + \int_{P_0}^{P} v_{IL}\, dP + h_0 \tag{6}$$

$$s_{IL} = \int_{T_0}^{T} \frac{c_{p,IL}}{T}\, dT + s_0 \tag{7}$$

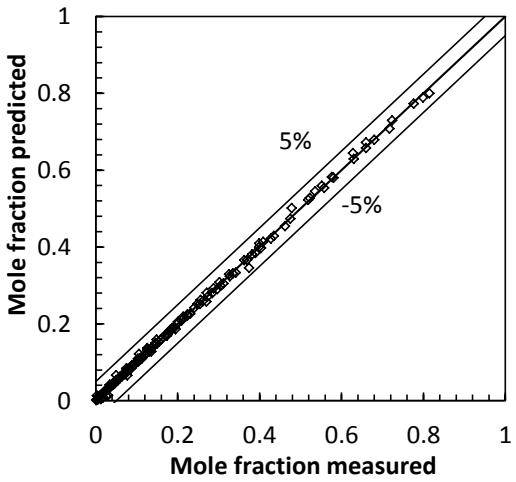

Figure 2: Comparison between the measured by Ren and Scurto (2006) and Seiler et al. (2004) and the predicted mole fractions using the NRTL model.

where $c_{p,IL}$ and v_{IL} are the specific heat and specific volume of the IL, and P is the pressure. The IIR reference state was adopted; h_0 = 200 kJ/kg and s_0 = 1kJ/kgK for the saturated liquid at T_0 = 0°C ($P_0 = P_{sat}(T_0)$). Then, the mixture enthalpy, H, and entropy, S, were calculated from Equation 8.

$$H = H^{id} + H^{E} \quad \text{and} \quad S = S^{id} + S^{E} \tag{8}$$

where the ideal solution properties of enthalpy, H^{id}, and entropy, S^{id}, can be obtained from Equation 9.

$$H^{id} = x_m H_m + x_n H_n \quad \text{and} \quad S^{id} = \left(x_m S_m + x_n S_n\right) - R\left(x_m \ln x_m + x_n \ln x_n\right) \tag{9}$$

The excess enthalpy, H^E, and excess entropy, S^E, can be calculated from Equations 10 and 11. (Shiflett and Yokozeki, 2006b)

$$H^{E} = -RT^{2}\left[x_m\left(\frac{\partial \ln \gamma_m}{\partial T}\right)_{P,x} + x_n\left(\frac{\partial \ln \gamma_n}{\partial T}\right)_{P,x}\right] \tag{10}$$

$$TS^{E} = H^{E} - G^{E} \tag{11}$$

where R is the universal gas constant and The excess Gibbs energy, G^E, can be calculated from Equation 12.

$$\frac{G^{E}}{RT} = x_m \ln \gamma_m + x_n \ln \gamma_n \tag{12}$$

2.3 First Law of Thermodynamic Analysis

Since the feasibility and the compatibility of ILs as an absorbent in an absorption system, in combination with refrigerants are the principal foci in this study, the performance of the system with respect to the refrigerant/IL mixtures is thermodynamically evaluated as a function of operating conditions.

Given the degree of subcooling at the condenser outlet, degree of superheat at the evaporator outlet, and the saturation temperatures for the condenser and evaporator, the condenser and evaporator outlet states (states 4 and 2) can be determined. Isenthalpic throttling through both the refrigerant and solution expansion devices is assumed resulting in Equations 13 and 14.

$$h_1 = h_4 \tag{13}$$

$$h_{10} = h_9 \tag{14}$$

The subscript numbers denote the states indicated in Fig. 1. The energy balance at the evaporator yields the refrigerant mass flow rate, Equation 15.

$$\dot{m}_{\mathrm{r}} = \frac{\left(h_2 - h_1\right)}{Q_{\mathrm{e}}} \tag{15}$$

The maximum desorber outlet temperature, T_8, and the absorber outlet temperature, T_5, are adjustable parameters which determine the refrigerant mass fractions of the strong ($x_s^m = x_5^m$) and weak solutions ($x_w^m = x_8^m$). The solution mass flow rates can be determined from Equations 16 and 17.

$$\dot{m}_{\mathrm{s}} = \dot{m}_{\mathrm{r}} \frac{\left(1 - x_w^m\right)}{\left(x_s^m - x_w^m\right)} \tag{16}$$

$$\dot{m}_{\mathrm{w}} = \dot{m}_{\mathrm{s}} - \dot{m}_{\mathrm{r}} \tag{17}$$

The subscripts "s" and "w" represent the strong- and weak-refrigerant solutions, respectively. Also, by assuming thermal equilibrium at the desorber outlet, $T_3 = T_8$, the heat transfer rate at the condenser can be calculated from Equation 18.

$$Q_{\mathrm{c}} = \dot{m}_{\mathrm{r}}\left(h_3 - h_4\right) = \dot{m}_{\mathrm{c,2nd}}\left(h_{12} - h_{11}\right) \tag{18}$$

The pumping process is assumed to be isentropic, yielding Equation 19.

$$s_6 = s_5 \tag{19}$$

The energy balances at the solution heat exchanger, assuming no heat losses to the environment, is expressed by Equation 20.

$$Q_{\mathrm{shx}} = \dot{m}_{\mathrm{s}}\left(h_7 - h_6\right) = \dot{m}_{\mathrm{w}}\left(h_8 - h_9\right) \tag{20}$$

where Q_{shx} is the heat transfer from the high temperature weak solution to the low temperature strong solution in the heat exchanger. The energy balances at the desorber and absorber is given by Equations 21 and 22.

$$Q_{\mathrm{d}} = \dot{m}_{\mathrm{w}}h_8 + \dot{m}_{\mathrm{r}}h_3 - \dot{m}_{\mathrm{s}}h_7 = \dot{m}_{\mathrm{d,2nd}}\left(h_{15} - h_{16}\right) \tag{21}$$

$$Q_{\mathrm{a}} = \dot{m}_{\mathrm{w}}h_{10} + \dot{m}_{\mathrm{r}}h_2 - \dot{m}_{\mathrm{s}}h_5 = \dot{m}_{\mathrm{a,2nd}}\left(h_{14} - h_{13}\right) \tag{22}$$

where Q_a is the heat removed from the refrigerant/IL mixture at the absorber. The pumping work W_p can be determined by Equation 23.

$$W_p = \dot{m}_{\mathrm{s}}\left(h_6 - h_6\right) \tag{23}$$

2.4 Second Law of Thermodynamic (Exergy) Analysis

Although above analysis based on the first law of thermodynamics determines the amount of energy entering and leaving from each one of the components as well as the entire system; however, it does not give information about energy quality, neither irreversibilities in the components and the complete system (Riveral et al., 2011). Exergy is defined as the amount of work available from an energy source. The maximum amount of work is obtainable when matter and/or energy such as thermal energy is brought to a state of thermodynamic equilibrium with the common components of the environment in which this process takes place with the dead state by means of a reversible process. The exergy content for an open, steady and non-reacting system can be expressed by Equations 24 (Moran and Sciubba, 1994).

$$Ex = \dot{m}\left(h - h_{ref}\right) - \dot{m}T_{ref}\left(s - s_{ref}\right) \tag{24}$$

where T_{ref} is the reference environmental temperature and h_{ref} and s_{ref} are specific enthalpy and entropy evaluated at the reference environmental state. Exergy is a measurement of how far a certain system deviates from a state of equilibrium with its environment. In general, exergy is not conserved. Every thermodynamic process is accompanied by certain type of irreversibilities which leads to exergy destruction of the process or to an increased consumption of energy (Christopher and Dimitrios, 2012). Thus, exergy analysis gives information about the irreversibilities of thermodynamic processes under consideration in terms of 'exergy loss', which suggests the possibilities that the process can be improved. *ex* in Eq. 23 is the physical specific exergy. The magnitude of the exergy involved with the heat transfer process, Ex_Q, is the work that could be obtained using a reversible Carnot cycle operating between the temperature from which the heat is received and the ambient temperature, yielding Equation 25.

$$Ex_Q = \left(1 - \frac{T_{ref}}{T}\right)Q \tag{25}$$

The bracketed term is exergy quality, which increases with the increasing temperature *T*. Then, the exergy loss, or irreversibility *I*, can be written as Equation 26.

$$I = \sum Ex_{in} - \sum Ex_{out} + \sum Q\left(1 - \frac{T_{ref}}{T}\right) - W \tag{26}$$

Following the Eq. 26, the exergy losses of the components in Fig. 1 can be determined by Equations 27 – 34.

$$I_e = Ex_1 - Ex_2 + Q_e\left(1 - \frac{T_{ref}}{T_{chip}}\right) \tag{27}$$

$$I_c = Ex_4 - Ex_1 + Ex_{11} - Ex_{12} \tag{28}$$

$$I_a = Ex_2 + Ex_{10} - Ex_5 + Ex_{13} - Ex_{14} \tag{29}$$

$$I_d = Ex_7 - Ex_8 - Ex_4 + Ex_{15} - Ex_{16} \tag{30}$$

$$I_{shx} = Ex_6 - Ex_7 + Ex_8 - Ex_9 \tag{31}$$

$$I_p = Ex_5 - Ex_6 + W_p \tag{32}$$

$$I_{evr} = Ex_4 - Ex_1 \tag{33}$$

$$I_{evs} = Ex_9 - Ex_{10} \tag{34}$$

The exergetic coefficient of performance can be defined as ratio of the exergy obtained at evaporator for cooling to the exergies supplied to desorber and pump, yielding Equation 35.

$$\text{ECOP} = \frac{Q_e\left(1 - T_{ref}/T_{chip}\right)}{Ex_{15} - Ex_{16} + W_p} \tag{35}$$

3. RESULTS & DISCUSSION

To be fully benefited by waste-heat, the maximum operating temperature of the absorption system should be lower than waste-heat temperature. Considering that the temperature of low grade waste-heat ranges 60-90°C, the maximum operating temperature of the system needs to be kept as low as possible. Fig. 3(a) shows ECOP variations with respect to the maximum operating temperature, i.e., desorber outlet temperature, T_8, where ECOP shows relatively sharp rise up to ~75°C followed by moderate decrease as the desorber outlet temperature rises beyond 75°C. The trend of ECOP is very close to that of COP shown in Kim et al. (2012). Water/[emim][BF_4] showed the best performance among the working fluids. The highest ECOP was around 0.97 at the desorber outlet temperature of 70°C. The better compatibility of water with [emim][BF_4] and the superior properties of water as a heat transfer fluid, such as large latent heat of evaporation, followed by extremely small refrigerant (water) flow rate resulted in its high performance (Kim et al., 2012). [R32, R134a and R152a showed moderate performances while R125 and R143a as the working fluid pairs of [bmim][PF_6] seem to be not acceptable.

The mole fractions of weak and strong solutions can be approximated using Equations 36 and 37, respectively.

$$x_w \sim \frac{P_c}{\gamma_w P_{sat}(T_8)} \tag{36}$$

$$x_s \sim \frac{P_e}{\gamma_s P_{sat}(T_5)} \tag{37}$$

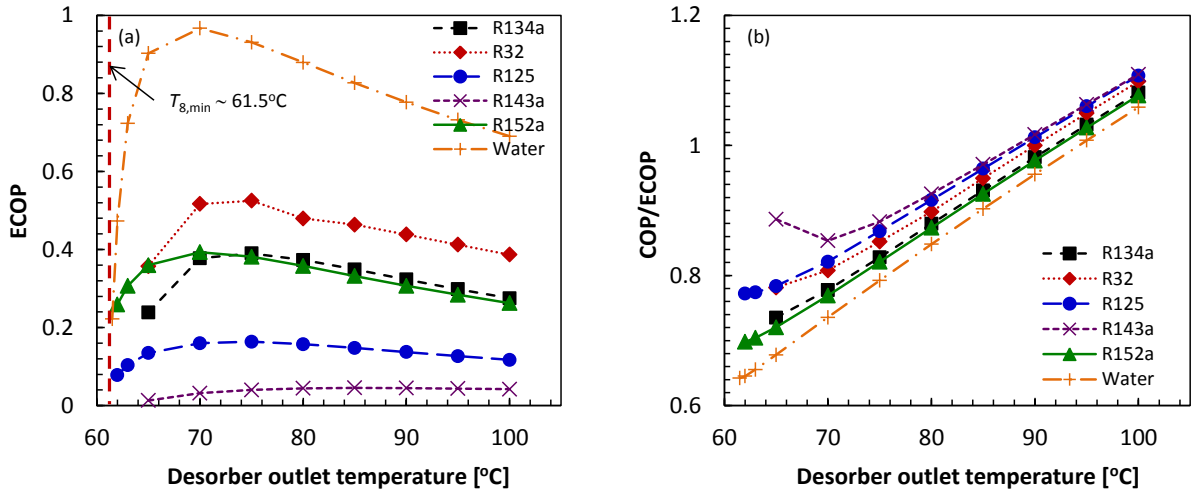

Figure 3: (a) ECOPs and (b) the ratio of COP to ECOP of the absorption system with respect to the desorber outlet temperature using different working fluid pairs: R134a/[bmim][PF_6], R32/[bmim][PF_6], R125/[bmim][PF_6], R143a/[bmim][PF_6], R152a/[bmim][PF_6], and water/[emim][BF_4].

Assuming $\gamma_s \approx \gamma_w$, Eqs. 36 and 37 can be written to yield Equations 38 and 39 using the inequality, $x_s > x_w$.

$$P_{\text{sat}}\left(T_8\right) > \frac{P_c}{P_e} P_{\text{sat}}\left(T_5\right) \tag{38}$$

$$T_8 > T_{\text{sat}}\left(\frac{P_c}{P_e} P_{\text{sat}}\left(T_5\right)\right) \sim T_{8,\min} \tag{39}$$

From Eq. 34, it can be seen that the lower bound on the desorber outlet temperature, or maximum operating temperature of the system, is a function of the operating conditions, i.e., vapor pressures at the evaporator and condenser as well as the absorber outlet temperature. Fig. 3(a) also shows that the ECOP curves generally converge to zero at $T_8 \sim 61.5^{\circ}$C (dashed line) for all refrigerants. Thus, the ECOP curves can be shifted to lower temperatures by adjusting the operating conditions so as to have optimum performance at a lower temperature, ca. 60°C. Then, the utilization of waste-heat can be optimized.

Fig. 3(b) shows the ratio of COP to ECOP. Assuming that the pumping work, W_p, is negligibly small, the definition of ECOP can be rewritten by Equation 40.

$$\text{ECOP} \approx \frac{Q_e\left(1-T_{ref}/T_{chip}\right)}{Ex_{15}-Ex_{16}} = \frac{Q_e\left(1-T_{ref}/T_{chip}\right)}{\dot{m}_{d,2nd}\left(h_{15}-h_{16}\right)-\dot{m}_{d,2nd}T_{ref}\left(s_{15}-s_{16}\right)} \tag{40}$$

The second law thermodynamics can be applied to the entropy difference in the denominator in Eq. 40 yielding Equation 41.

$$\dot{m}_{d,2nd}T_{ref}\left(s_{15}-s_{16}\right) = \frac{Q_d}{T_{d,rev}} + \theta_d \equiv \frac{Q_d}{T_{d,irr}} \tag{41}$$

where θ_d is the entropy generation at secondary fluid of desorber during heat transfer and $T_{d,rev}$ and $T_{d,irr}$ are the characteristic desorber heat transfer temperatures for reversible and irreversible processes, respectively. Then, using Eqs. 21 and 41, the ECOP can be related to COP, Equation 42.

$$\text{ECOP} \approx \frac{Q_e\left(1-T_{ref}/T_{chip}\right)}{Q_d\left(1-T_{ref}/T_{d,irr}\right)} \approx \text{COP}\frac{1-T_{ref}/T_{chip}}{1-T_{ref}/T_{d,irr}} \tag{42}$$

Thus, ECOP is modified COP by the ratio of exergy qualities at the desorber temperature to chip temperature. Fig. 3(b) shows that as the desorber outlet temperature increases, the COP to ECOP ratio increases.

Fig. 4 shows the total cycle irreversibilities of the absorption system. As expected, remarkably large irreversibility is

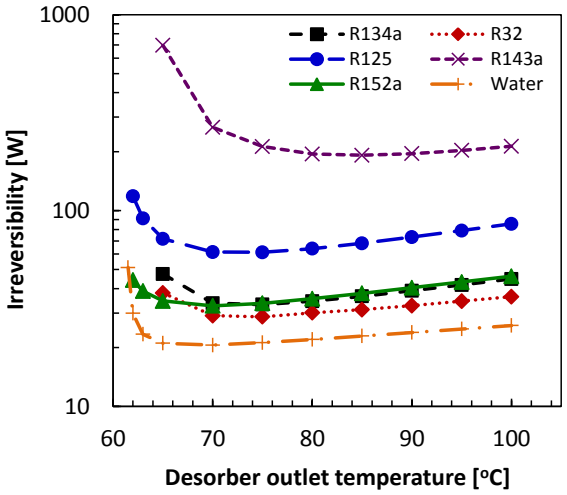

Figure 4: Total cycle irreversibilities of the absorption system with respect to the desorber outlet temperature using different working fluid pairs: R134a/[bmim][PF_6], R32/[bmim][PF_6], R125/[bmim][PF_6], R143a/[bmim][PF_6], R152a/[bmim][PF_6], and water/[emim][BF_4].

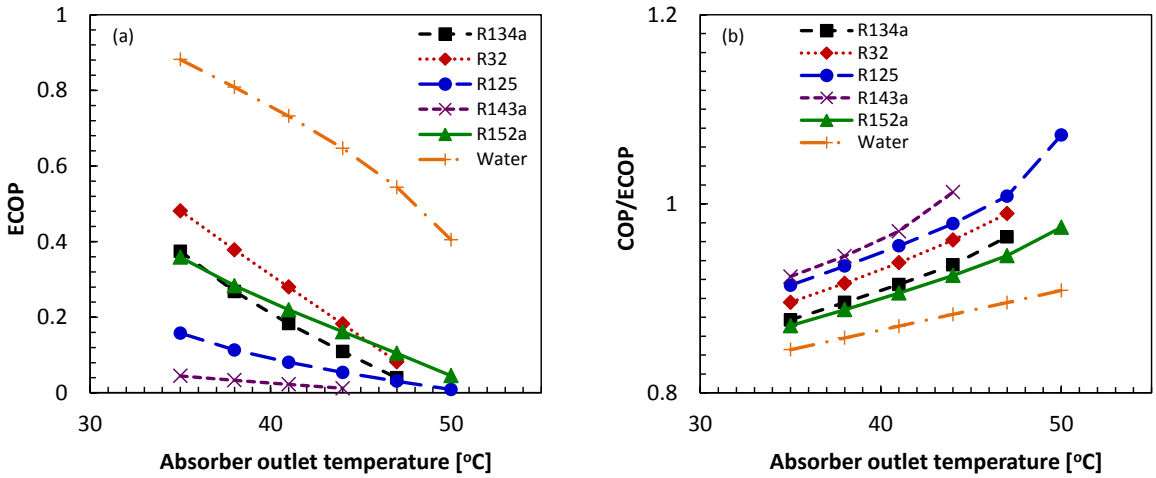

Figure 5: (a) ECOPs and (b) the ratio of COP to ECOP of the absorption system with respect to the absorber outlet temperature using different working fluid pairs: R134a/[bmim][PF6], R32/[bmim][PF6], R125/[bmim][PF6], R143a/[bmim][PF6], R152a/[bmim][PF6], and water/[emim][BF_4].

brought by R143a/[bmim][PF_6], while that of water/[emim][BF_4] is the smallest among the working fluids. It is clear that the ECOP trend with respect to working fluid in Fig. 3(a) is direct outcome of the exergy losses in Fig. 4.

Fig. 5(a) shows the effects of absorber outlet temperature on ECOP. Absorber outlet temperature is determined and adjusted by the ambient cooling temperature. As shown in Fig (5), lower absorber outlet temperature enhances the system performance in terms of ECOP. Also, the performance of water/[emim][BF_4] is superior to other working fluids. In Fig. 5(b), increase in the absorber outlet temperature resulted in relative increase of COP to ECOP ratio. The desorber outlet temperature was maintained at 80°C, however the desorber inlet temperature, T_7, is increased by increase of absorber outlet temperature. As a consequence, smaller temperature difference between desorber secondary fluid inlet and outlet, i.e., T_{15} and T_{16}, was accompanied. Since $T_{d,irr} \sim 0.5(T_{15}+T_{16})$, $T_{d,irr}$ rises along with the increase of absorber outlet temperature. Therefore, following Eq. 42, the ratio in Fig. 5(b) increases with the increasing absorber outlet temperature.

Irreversibilities of absorption system components are depicted in Fig. 6. At low temperature, the large cycle irreversibility is mainly attributed to the large exergy loss in solution expansion valve (39.3% of total irreversibility). The exergy loss in solution expansion valve is rapidly reduced with increasing desorber outlet temperature. However, the irreversibilities of other components such as absorber, desorber and condenser are increasing, which leads to the gradual increase of irreversibility and thus the lowering of ECOP in Fig. 3(a). The irreversibility of evaporator is considerably large, which indicates the improvement potential by adjusting (lowering) the chip temperature.

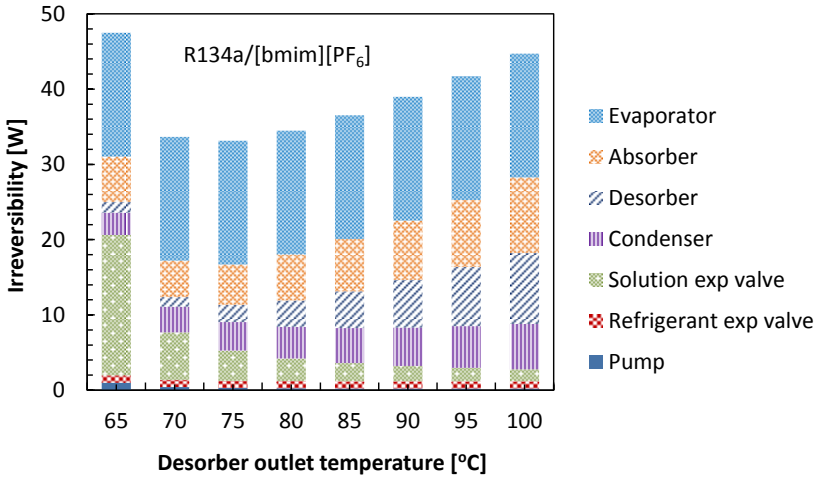

Figure 6: Irreversibilities of absorption system components with respect to desorber outlet temperature with R134a/[bmim][PF_6] as working fluid.

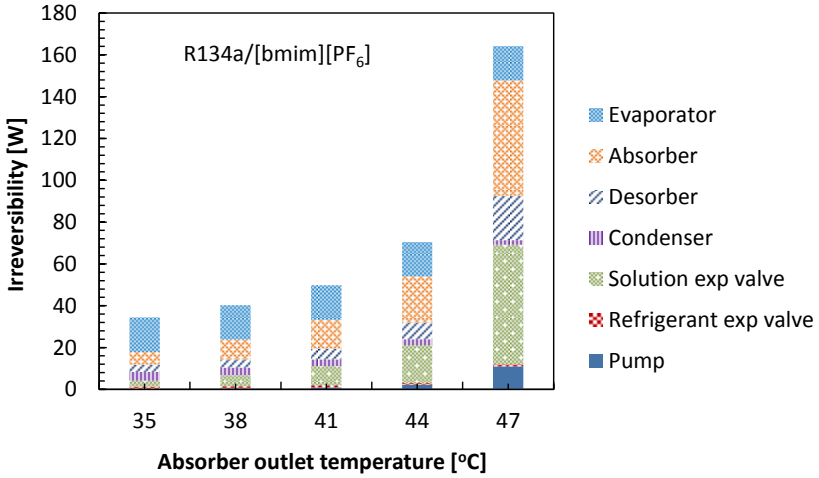

Figure 7: Irreversibilities of absorption system components with respect to absorber outlet temperature with R134a/[bmim][PF_6] as working fluid.

Fig. 7 shows the effect of absorber outlet temperature on the components irreversibilities. As the absorber outlet temperature increases, significant increases in absorber and solution expansion exergy losses are observed, while the increase of the desorber exergy loss increase is relatively slower. The increase of solution expansion valve irreversibility is mainly resulted from the increase solution flow rate caused by the reduction of strong solution mole fraction, $x_5 = x_s$, approaching weak solution mole fraction, $x_8 = x_w$.

CONCLUSION

The various mixtures of refrigerant/IL as working fluid of absorption refrigeration system were explored using first and second law thermodynamic analysis. NRTL model is built and used to predict the solubility of the mixtures. The performance analysis showed that the ECOP of water/[emim][BF_4] was superior to those of other working fluids. It is attributed to the better compatibility of water with [emim][BF_4] and the superior properties of water as a heat transfer fluid, such as large latent heat of evaporation, followed by extremely small refrigerant (water) flow rate resulted in its high performance. However, the temperature range of water as refrigerant is not acceptable for low temperature applications. It is verified that the system irreversibility directly affect the system performance in terms of ECOP. The trend of ECOP observed in this study was very close to that of COP in Kim et al. (2012). The system level numerical investigation showed that IL as a working fluid is promising and but there is possibilities of performance improvements by reducing the irreversibilities. In the future, the system performance needs to be experimentally demonstrated, novel and efficient microfluidic absorber and desorber need to be developed and low pressure, high solubility IL/refrigerants combination needs to be investigated.

NOMENCLATURE

C	Lockhart and Martinelli correlation coefficient	
COP	coefficient of performance	
COP_{waste}	coefficient of performance with waste-heat	
c_p	specific heat	(J/kgK)
d_h	hydraulic diameter	(m)
Ex	exergy	(W)
ECOP	exergetic coefficient of performance	
F	adjustable binary interaction parameter	
f	fanning friction factor	
G	Gibbs energy	(J)
G_m	mass flux	(kg/m^{2}s)
H	enthalpy	(J)
h	specific enthalpy	(J/kg)

Greek Symbols

β	aspect ratio	
ε	void fraction	
θ	entropy generation	(J/kgK)
γ	activity coefficient	
μ	viscosity	(Pa·s)
ρ	density	(kg/m^3)
τ	adjustable parameters of Eq. 5	
ϕ	two-phase multiplier	

Subscripts

0	reference state
1, …, 16	state numbers indicated in Fig. 1

I	irreversibility	(W)	2nd	2ndary fluid
M	molecular weight	(kg/mol)	a	absorber
$\dot{m}$	mass flow rate	(kg/s)	c	condenser
P	pressure	(Pa)	chip	chip
Q	heat transfer	(W)	d	desorber
R	gas constant, 8.314 J/mol·K		e	evaporator
IL	ionic-liquid		evr	refrigerant expansion valve
Re_{lo}	liquid-only Reynolds number		evs	solution expansion valve
S	entropy	(J/K)	in	inlet
s	specific entropy	(J/kg·K)	irr	irreversible
T	temperature	(K)	l	liquid
v	specific volume	(m^3/kg)	out	outlet
We_{lo}	liquid-only Weber number			
W_p	pumping work	(W)	p	pump
X	Martinelli parameter		r	refrigerant
x	liquid phase refrigerant mole fraction		ref	reference state
x_m	liquid phase refrigerant mole fraction		rev	reversible
x^m	liquid phase refrigerant mass fraction		s	strong-refrigerant solution
x_n	liquid phase ionic-liquid mole fraction		sat	saturation
x^v	vapor quality		shx	solution heat exchanger
z	coordinate	(m)	v	vapor
			w	weak-refrigerant solution
			v	vapor

Superscripts

E	excess property
id	ideal solution

REFERENCES

Bintoro, J.S., Akbarzadeh, A., and Mochizuki, M., 2005, A closed-loop electronics cooling by implementing single phase impinging jet and mini channels heat exchanger, Appl. Therm. Eng., vol. 25: p. 2740-2753.

Blake, D.M., Moens, L., Rudnicki, D., and Pilath, H., 2006, Lifetime of imidazolium salts at elevated temperatures, J. Sol. Energy Eng., vol. 128: p. 54-57.

Christopher, K. and Dimitrios, R., 2012, A review on exergy comparison of hydrogen production methods from renewable energy sources, Energy. Environ. Sci., vol. 5: p. 6640-6651.

Cull, S.G., Holbrey, J.D., Vargas-Mora, V., Seddon, K.R., and Lye, G.J., 2000, Room-temperature ionic liquids as replacements for organic solvents in multiphase bioprocess operations, Biotechnol. Bioeng., vol. 69, no. 2: p. 227-233.

Drost, M.K. and Friedrich, M., 1997, Miniature heat pump for portable and distributed space conditioning applications. Proc. the 32nd Intersociety Energy Conversion Engineering Conference: p.1271-1274.

Dzyuba, S.V. and Bartsch, R.A., 2002, Influence of structural sariations in1-alkyl(aralkyl)-3-methylimidazolium hexafluorophosphates and bis(trifluoromethylsulfonyl)imides on physical properties of the ionic liquids, Chem. Phys. Chem., vol. 3: p. 161-166.

Fan, X., Zeng, G., LaBounty, C., Bowers, J.E., Croke, E., Ahn, C.C., Huxtable, S., Majumdar, A., and Shakouri, A., 2001, SiGeC/Si superlattice microcoolers, Appl. Phys. Lett., vol.78, no. 11: p. 1580-1582.

Gardas, R.L. and Coutinho, J.A.P., 2008, A group contribution method for heat capacity estimation of ionic liquids, Ind. Eng. Chem. Res., vol. 47, no. 15: p. 5751-5757.

Gardas, R.L. and Coutinho, J.A.P., 2009, Group contribution methods for the prediction of thermophysical and transport properties of ionic liquids, AIChE Journal, vol. 55, no. 5: p. 1274-1290.

Hagiwara, R. and Ito, Y., 2005, Room temperature ionic liquids of alkylimidazoliumcations and fluoroanions, J. Fluorine. Chem., vol. 105: p. 221–227.

Heintz, A., Lehmann, J.K., and Wertz, C., 2003, Thermodynamic properties of mixtures containing ionic liquids. 3. liquid-liquid equilibria of binary mixtures of1-ethyl-3-methylimidazolium bis(trifluoromethylsulfonyl)imide with propan-1-ol, butan-1-ol, and pentan-1-ol, J. Chem. Eng. Data., vol. 48: p. 472-474.

Huddleston, J.G., Visser, A.E., Reichert, W.M., Willauer, H.D., Broker, G.A., and Rogers, R.D., 2001, Characterization and comparison of hydrophilic and hydrophobic room temperature ionic liquids incorporating the imidazolium cation, Green Chem., vol. 3: p. 156–164.

Huddleston, J.G., Willauer, H.D., Swatloski, R.P., Visser, A.E., and Rogers, R.D., 1998, Room temperature ionic liquids as novel media for 'clean' liquid–liquid extraction, Chem. Commun., vol. 34, no. 16: p. 1765-1766.

Ibrahim, O.M. and Klein, S.A., 1996, Absorption power cycles, Energy, vol. 21, no. 1: p. 21-27.

International Technology Roadmap for Semiconductors, Assembly and Packaging, 2005 Ed.

Jacquemin, J., Husson, P., Mayer, V., and Cibulka, I., 2007, High-pressure volumetric properties of imidazolium-based ionic liquids: effect of the anion, J. Chem. Eng. Data., vol.52: p. 2204-2211.

Jiang, L., Mikkelsen, J., Koo, J.M., Huber, D., Yao, S., Zhang, L., Zhou, P., Maveety, J.G., Prasher, R., Santiago, J.G., Kenny, T.W., and Goodson, K.E., 2002, Closed-loop electroosmotic microchannel cooling system for VLSI circuits, IEEE Trans. Comp. Pack. Tech. vol. 25, no. 3: p. 347-355.

Kim, Y.J., Joshi, Y.K., and Fedorov, A.G., 2008, An absorption miniature heat pump system for electronics cooling, Int. J. Regrig., vol. 31, no. 1: p. 23-33.

Kim, S., Kim, Y.J., Joshi, Y.K., Fedorov, A.G., and Kohl, P.A., 2011a, Absorption heat pump/refrigeration system utilizing ionic liquid and hydrofluorocarbon refrigerants, submitted to Applied Energy.

Kim, Y.J., Kim, S., Joshi, Y.K., Fedorov, A.G., and Kohl, P.A., 2011b, Waste-heat driven miniature absorption refrigeration system using ionic-liquid as a working fluid, Proc. the 5th International Conference on Energy Sustainability; ESFuelCell2011-54217.

Kim, Y.J., Kim, S., Joshi, Y.K., Fedorov, A.G., and Kohl, P.A., 2012, Thermodynamic analysis of an absorption refrigeration system with ionic-liquid/refrigerant mixture as a working fluid, Accepted to be published in Energy.

Marsh, K.N., Boxall, J.A., and Lichtenthaler, R., 2004, Room temperature ionic liquids and their mixtures - a review, Fluid Phase Equilibr., vol. 219: p. 93-98.

Maydanik, Y.F., Vershinin, S.V., Korukov, M.A., and Ochterbeck, J.M., 2005, Miniature loop heat pipes-a promising means for electronics cooling, IEEE Trans. Comp. Pack. Tech. vol. 28, no. 2: p. 290-296.

McLinden, M.O., Klein, S., Lemmon, E., and Peskin, A., 1998, NIST thermodynamic and transport properties of refrigerants and refrigerant mixtures database (REFPROP), Version 6.0, National Institute of Standards and Technology, Gaithersburg, MD.

Mongia, R., Masahiro, K., DiStefano, E., Barry, J., Chen, W., Izenson, M., Possamai, F., Zimmermann, A., and Mochizuki, M., 2006, Small scale refrigeration system for electronics cooling within a notebook computer, Proc. the 10th Intersociety Conference on Thermal and Thermomechanical Phenomena in Electronics Systems: p. 751-758.

Moran, M.J. and Sciubba, E., 1994, Exergy analysis: principles and practice, J. Eng. Gas Turb. Power, vol. 116: p. 285-290.

Pal, A., Joshi, Y.K., Beitelmal, M.H., Patel, C.D., and Wenger, T.M., 2002, Design and performance evaluation of a compact thermosyphon, IEEE Trans. Comp. Pack. Tech., vol. 25, no. 4: p. 601-607.

Ren, W. and Scurto, A.M., 2009, Phase equilibria of imidazolium ionic liquids and the refrigerant gas, 1,1,1,2-tetrafluoroethane (R-134a), Fluid Phase Equilibr., vol. 286: p. 1-7.

Rivera, W., Huicochea, A., Martínez, H., Siqueiros, J., Juárez, D., and Cadenas, E., 2011, Exergy analysis of an experimental heat transformer for water purification, Energy, vol. 36, no. 1: p. 320–327.

Rogers, R.D. and Seddon, K.R., 2003, Ionic liquids – solvents of the future?, Science, vol. 302: p. 792-793.

Scammells, P.J., Scott, J.L., and Singer, R.D., 2004, Ionic liquids: The neglected issues, Aust. J. Chem., vol. 58: p. 155-169.

Seiler, M., Jork, C., Kavarnou, A., Arltet, W., and Hirsch, R., 2004, Separation of azeotropic mixtures using hyperbranched polymers or ionic liquids, AIChE Journal, vol. 50, no. 10: p. 2439-2454.

Shiflett, M.B. and Yokozeki, A., 2006a, Absorption cycle utilizing ionic liquid as working Fluid, US Patent, 0197053: p. 1-47.

Shiflett, M.B. and Yokozeki, A., 2006b, Solubility and diffusivity of hydrofluorocarbons in room-temperature ionic liquids, AIChE Journal, vol. 52, no. 3: p. 1205-19.

Shiflett, M.B. and Yokozeki, A., 2007, Utilizing ionic liquids for hydrofluorocarbon separation, US Patent, 0131535: p. 1-42.

Smith, J.M., Van Ness, H.C., and Abbott, M., 2000, Introduction to Chemical Engineering Thermodynamics. 6th ed., McGraw-Hill, New York.

Sun, ZG., 2008, Experimental investigation of integrated refrigeration system (IRS) with gas engine, compression chiller and absorption chiller, Energy, vol. 33: p. 431–436.

Swatloski, R.P., Spear, S.K., Holbrey, J.D., and Rogers, R.D., 2002, Dissolution of cellose with ionic liquids, J. Am. Chem. Soc., vol. 124, no. 18: p. 4974-4975.

Troncoso, J., Cerdeirina, C.A., Sanmamed, Y.A., Romani, L., and Rebelo, L.P.N., 2006, Thermodynamic properties of imidazolium-based ionic liquids: densities, heat capacities, and enthalpies of fusion of [bmim][PF_6] and [bmim][NTf_2], J. Chem. Eng. Data., vol. 51: p. 1856-1859.

Valkenburg, M.E.V., Vaughn, R.L., Williams, M., and Wilkes, J.S., 2005, Thermochemistry of ionic liquid heat-transfer fluids, Thermochim. Acta, vol. 425: p. 181–188.

Wasserscheid, P. and Keim, W., 2000, Ionic liquids - new solutions for transition metal catalysis, Angewandte. Chemie. International Edition, vol. 39: p. 3772-3789.

Wei, Y. and Joshi, Y.K., 2004, Stacked microchannel heat sinks for liquid cooling of microelectronic components, J. Electron. Pack., vol. 126: p. 60-66.

Wilkes, J.S., 2004, Properties of ionic liquid solvents for catalysis, J. Mol. Catal. A: Chem., vol. 214: p. 11–17.

Xu, F., Goswami, D.Y., and Bhagwat, S.S., 2000, A combined power/cooling cycle, Energy, vol. 25: p. 233–246.

Yokozeki, A., 2005, Theoretical performances of various refrigerant-absorbent pairs in a vapor-absorption refrigeration cycle by the use of equations of state, Applied Energy, vol. 80, no. 4: p. 383-399.